AEROSPACE REPORT NO.
ATR-2018-00953

Comparison of Modeling Techniques for Radiation Dose in a Realistic Geometry

January 14, 2018

Mark D. Looper
Magnetospheric and Heliospheric Sciences
Space Sciences Department

Prepared for:

Senior Vice President, Engineering and Technology Group

Authorized by: Engineering and Technology Group

Acknowledgments

The author thanks Can Q. Nguyen for help in format conversion of the REACH CAD files, and Joseph E. Mazur for numerous discussions about the REACH hardware and its accommodation aboard the host spacecraft. This work was supported by the Aerospace Technical Investment Program (ATIP) under a Long Term Capability Development (LTCD) project, JO 6416-01.

Abstract

The Geant4 open-source radiation transport code package provides a variety of ways to model the response to the space radiation environment of sensitive parts or detectors embedded in inert shielding or structural material. The simulated geometry can be built in the C++ user code entirely from primitive solid shapes (boxes, cones, etc.), or portions can be imported from CAD (computer-aided design) files. The nominal radiation transport technique provided is a forward Monte Carlo simulation, which provides the best accuracy; for increased simulation speed with some reduction in realism of modeled physical processes, recent versions of Geant4 have also enabled adjoint Monte Carlo simulations, and we have also used Geant4 to implement a variant of the sector shielding technique with some improvements over the standard technique. In this report we compare the results of dose calculations employing various combinations of these capabilities (with vs. without CAD import of some of the geometry, and forward vs. adjoint Monte Carlo techniques vs. sector shielding) for protons and electrons irradiating a realistic geometry representing our REACH microdosimeter payload and a portion of its host spacecraft. We find that using CAD import to avoid constructing parts of the geometry by hand-coded C++ gives results that agree with the fully hand-built geometry, but that runtimes are significantly longer. The adjoint Monte Carlo technique provides a great increase in speed, and results agree well with those from forward simulations for electrons, but the present state of the proton adjoint simulations in Geant4 gives results that are too different from the forward results for us to use them. The improved sector shielding technique gives an even greater boost in speed for protons, and results agree well with those from forward Monte Carlo simulations.

Contents

Figures

1. Speeding Up Coding and Running of Geant4 Simulations

Geant4 [1] is an open-source toolkit to enable a user to simulate the transport of energetic-particle radiation through matter. It is very detailed, modeling the trajectories of individual particles through a user-defined geometry with user-chosen physics lists that can simulate a wide variety of electromagnetic or nuclear interactions. It is also very general, providing access to all properties (position, velocity, charge, energy deposit, etc.) of each particle at all points along its trajectory, so that the user can tabulate any quantities of interest from simple energy deposit (radiation dose) to complicated sensor backgrounds, production of secondary particles, etc.

The standard use of the code is to implement "forward" Monte Carlo simulations through a hand-coded geometry. The user defines the structure to be simulated using a wide variety of geometric "primitives" (G4Box, G4Sphere, G4Trap[ezoid], etc.) accessible in the C++ user code, then places them in the world volume and assigns materials, fields, etc. to them. Then individual particles are launched into and through the geometry, with such non-deterministic processes as nuclear interactions, scattering, energy-loss fluctuations, etc., being sampled randomly from the relevant probability distribution functions. With many simulated particles the ensemble exhibits realistic behavior, including rare occurrences like production of certain secondary particles, large-angle scattering, etc., that would not be captured in a tabulation of average particle behavior. See, e.g., Reference [5].

This thoroughness, however, comes at a high cost in time spent programming and running the code; it can take days or weeks to define and debug a complex geometry, and we routinely run simulations on hundreds of cluster cores for days at a time. Looper [4] evaluated alternatives to the standard Geant4 forward Monte Carlo technique, which would run much faster at some cost in physical realism. The "adjoint" Monte Carlo technique traces particles backward in time in a probabilistic sense and outward from a (typically small) sensitive volume inside the geometry, and an improved sector shielding technique traced proton trajectories to and through this sensitive volume while neglecting scattering, energy deposit fluctuations, and generation of secondary particles. Since both of these techniques focus only on particles that actually reach the sensitive volume, they require many fewer steps than a full forward simulation that typically illuminates the entire exterior of the simulation volume with particles representative of the space radiation environment.

The complex task of using Geant4 geometric primitives to hand-build the material structures to be modeled can also be sped up if a CAD (computer-aided design) representation of the geometry is available in an appropriate format and with an appropriate level of detail. Geant4 can read geometric shapes from files in the GDML format (Geometry Description Markup Language [2]), which can be created from standard CAD file formats like STEP using, e.g., FASTRAD (http://www.fastrad.net/). If such files are available, complex structures can be imported into Geant4 in a few lines of code instead of via numerous hand-built primitives; the same materials can be assigned to GDML-imported structures within a Geant4 user code as are available for hand-coded structures, and parts of the structure for which more detail is necessary or for which CAD files are not available can be built among and around the imported structures using Geant4 primitives, so that no flexibility is lost by using CAD import to save coding time.

However, because Geant4 uses tessellation of the surfaces of GDML structures to represent them internally, navigation within these structures can be very complex and tracking of particles through CAD-imported structures will be slower than through primitives (for which such things as the distance from a point inside a G4Box to its nearest boundary, for example, can be calculated analytically). Thus the time saved in coding the geometry comes at a cost in the form of extra time spent running the simulation. The purpose of this report is to evaluate combinations of these techniques, CAD import vs. hand-coded

geometry and forward vs. adjoint Monte Carlo vs. improved sector-shielding particle transport, to compare accuracy of results and computational speed. This will give us insight into the appropriate combination of techniques to use for calculations for which the standard use of Geant4, i.e., forward Monte Carlo particle transport simulations through a hand-built geometry, would require too much time to code and/or run.

2. Simulation Geometry and Baseline Results

A use case that is a good candidate for alternative modeling techniques is that of a small dosimeter embedded as a hosted payload within a much larger satellite. Aerospace is currently deploying the REACH dual microdosimeter payload inside a commercial satellite host in low Earth orbit (LEO). There are several configurations of REACH "pods"; a representative example, as modeled, is shown in a Geant4-generated image of the hand-built geometry in Figure 1. Two Aerospace-developed microdosimeters, with 3mm x 7mm x 250 micron silicon detector mounted inside a 1" x 1" Kovar package (see, e.g., [6]), are mounted to a circuit board (green) inside an aluminum housing (blue) and encased in thick Mallory shields (medium gray) with an opening above the detector. Left and right positions in the image are referred to as B and A. Each detector is surrounded by a Mallory shield (medium gray) and views space through a 4 mil window in the Kovar lid of the microdosimeter package (red), then through either 0, 23, 56, or 80 mils of Mallory window (dark gray); the pod is mounted on the inside surface of an external aluminum panel of the host enclosure, which is thinned to 20 mils above the detectors. The host provided us with CAD drawings of the structure that surrounds the REACH pod, including the panel to which the REACH pod is mounted; they are considered proprietary, and will not be reproduced herein. For the present comparison of techniques, only the panel (about 8" x 13") under which the pod is mounted and the structures attached to the top of the panel will be modeled; this subset of the geometry is small enough that a conventional forward Monte Carlo simulation through hand-coded geometry is feasible, so as to enable a comparison with other techniques. These two structures and the pod housing (blue in Figure 1) were either imported via STEP-to-GDML conversion or built by hand from Geant4 primitives; the circuit board and microdosimeter/shield structures were hand-coded and, as necessary, spliced into the CAD-imported structures. To close out the rear of the panel behind the REACH pod, a minimal aluminum box with 200 mil thick walls (approximating the minimum shielding thickness in any direction behind the panel) was hand-coded.

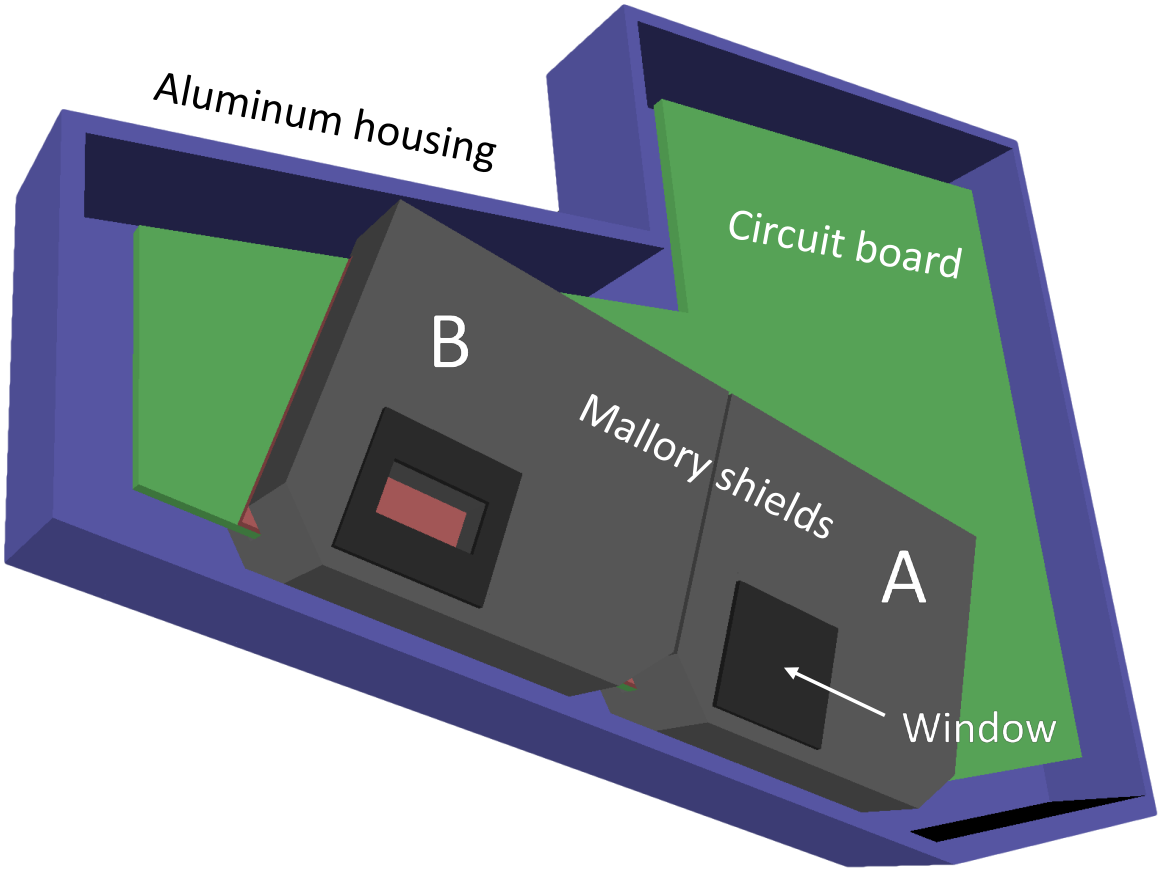

Figure 1. Geant4 geometry for a representative REACH microdosimeter pod. No Mallory window covers the left microdosimeter aperture (B position), and a window is present over the right aperture (A position). Red is the Kovar microdosimeter housing, green is the circuit board, blue is the aluminum pod, and light and dark gray are the Mallory shielding and window.

For the Geant4 simulations in this report we used a pod configuration with 0 mils of Mallory at position B and 56 mils at A, and a configuration with 23 mils at B and 80 mils at A. These shields are representative of actual REACH flight hardware but their specific locations (A or B) and combinations are not exact matches to REACH. All simulations herein were performed with Geant4 version 10.3, patch level 2 (geant4.10.03.p02); the forward Monte Carlo simulations used the Shielding_EMZ reference physics list, which models a very complete array of nuclear interactions and has electromagnetic models tuned for the lower energies (compared to particle accelerators) of interest in space. The results for the microdosimeter with 0 mils of Mallory are shown in Figure 2 through Figure 5, which display the energy deposit spectra as functions of the energy of the isotropically incident primary protons or electrons. The colorscale shows the logarithm of this response in units of cm^2 sr per MeV of energy deposit; this can be convolved in particle energy with a primary particle spectrum to give the resulting energy deposit spectrum. Figure 2 shows the response to protons coming in from above, i.e., the outer surface of the panel above the pod, and Figure 3 shows the response for protons coming from below, i.e., through the closeout box at the rear, while Figure 4 and Figure 5 show the same for electrons. The label “Forward MC/Primitives” indicates the simulation configuration, in this case a forward Monte Carlo with geometry built from Geant4 primitives.

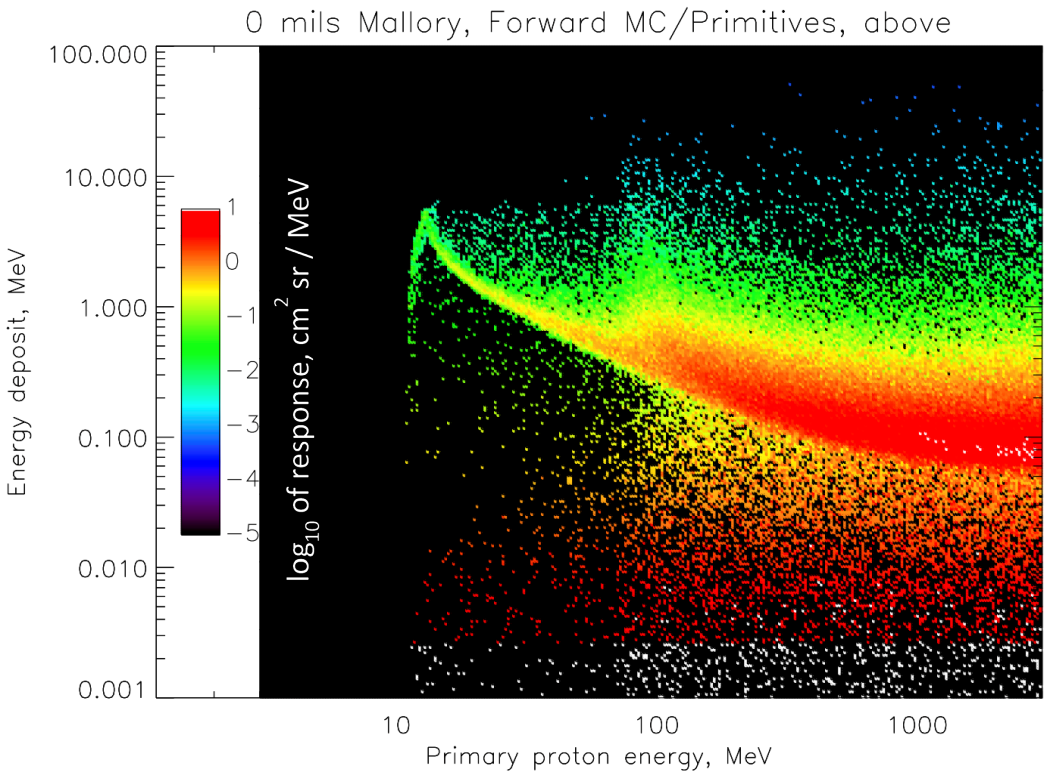

Figure 2. Energy deposit response to isotropically incident protons of microdosimeter without Mallory over aperture. "Forward MC/Primitives" indicates forward Monte Carlo simulation with geometry built entirely from Geant4 primitives; this plot is for the subset of protons coming in from above the top of the panel to which the REACH pod is mounted. Colorscale is logarithm of response in cm^2 sr per MeV of energy deposit.

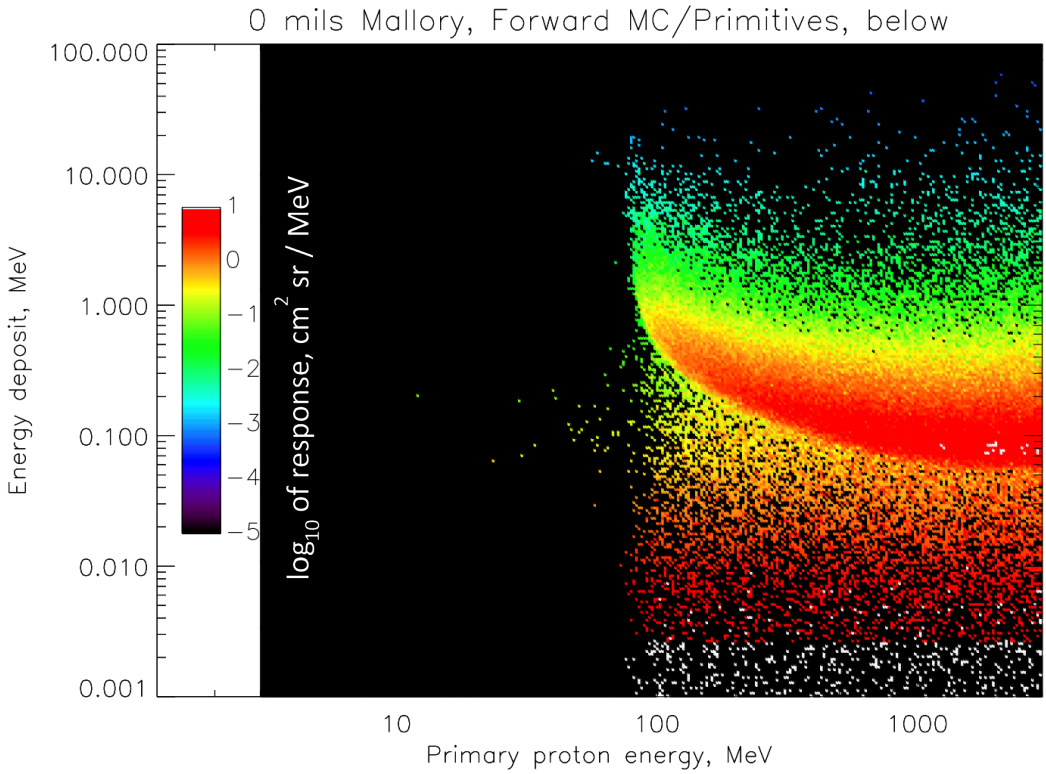

Figure 3. Energy deposit response to isotropically incident protons of microdosimeter without Mallory over aperture. This is the "Forward MC/Primitives" simulation configuration, for the subset of protons coming from the rear of the panel. Colorscale is the same as that in Figure 2.

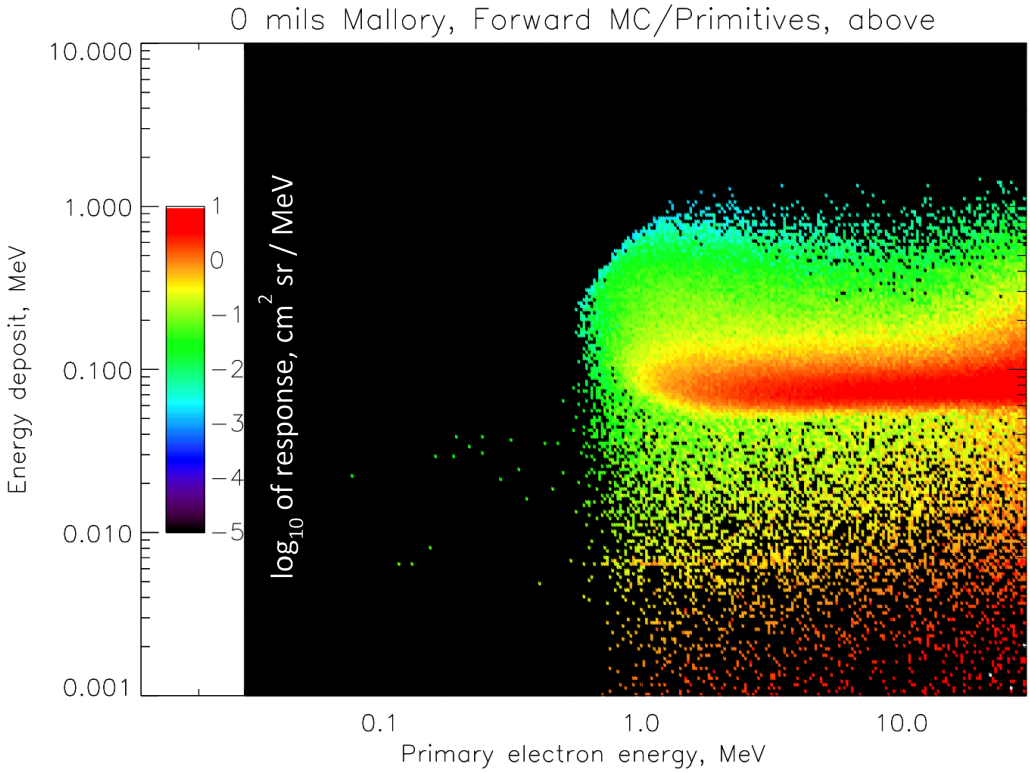

Figure 4. Energy deposit response to isotropically incident electrons of microdosimeter without Mallory over aperture. This is the "Forward MC/Primitives" simulation configuration, for the subset of electrons coming from the top of the panel. Colorscale is the same as that in Figure 2.

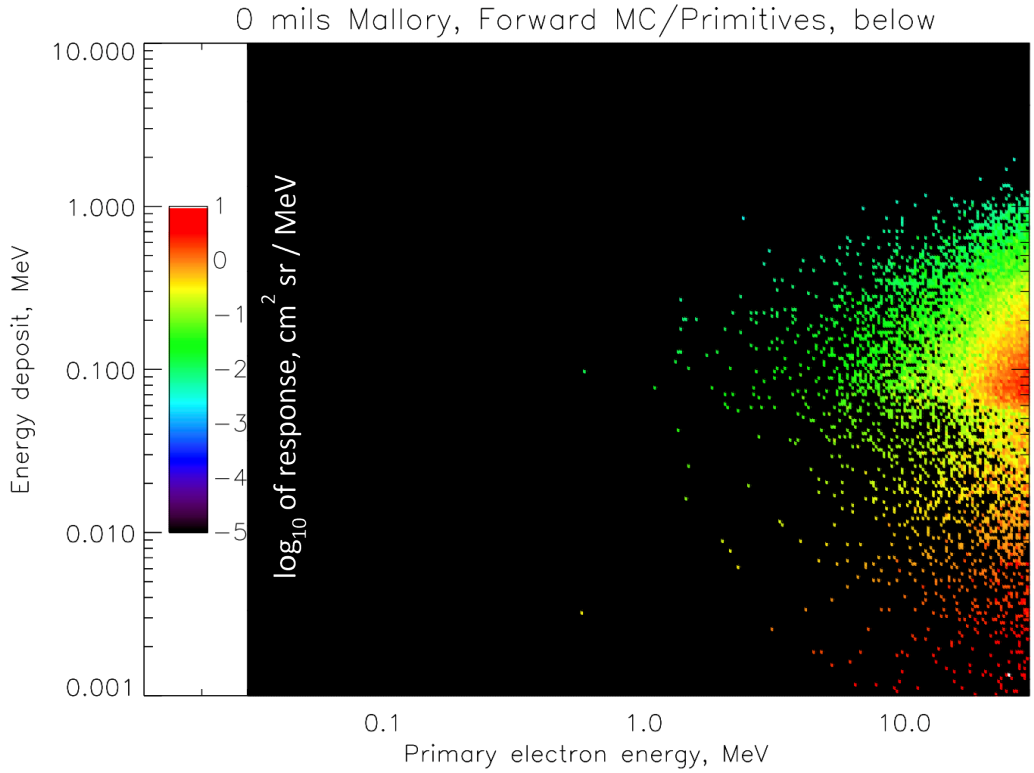

Figure 5. Energy deposit response to isotropically incident electrons of microdosimeter without Mallory over aperture. This is the "Forward MC/Primitives" simulation configuration, for the subset of electrons coming from the rear of the panel. Colorscale is the same as that in Figure 2.

Comparing the proton figures with those for the other three configurations of Mallory (23, 56, 80 mils), not shown, the "above" plots like Figure 2 are all similar above about 70 MeV, where protons start to penetrate the shielding around the aperture, with varying response below due to the different Mallory thicknesses that may be present in the aperture. All four "below" plots, not surprisingly, look very similar to Figure 3 since shielding is essentially identical for all microdosimeters on the side away from the panel surface, and protons start to penetrate it at about 80 MeV. For electrons, the response of all microdosimeters to electrons penetrating the shielding adjacent to the apertures from above starts around 20 MeV, so plots for other Mallory configurations look similar to Figure 4 above that energy, with lesser extensions to lower electron energy for thicker Mallory; again, plots for illumination from below look very much like Figure 5 in all cases.

Figure 6 and Figure 7 summarize the comparison of the four Mallory configurations, showing total dose response for illumination by protons and electrons from above and below. Integrating over a vertical strip through one of the plots in Figure 2 to Figure 5 and dividing by detector mass to convert energy deposit to dose would give a single point on one of Figure 6 or Figure 7; convolving one of these curves in energy with a proton or electron spectrum in particles per (cm^2 sr sec MeV) would give a dose rate in rads per second.

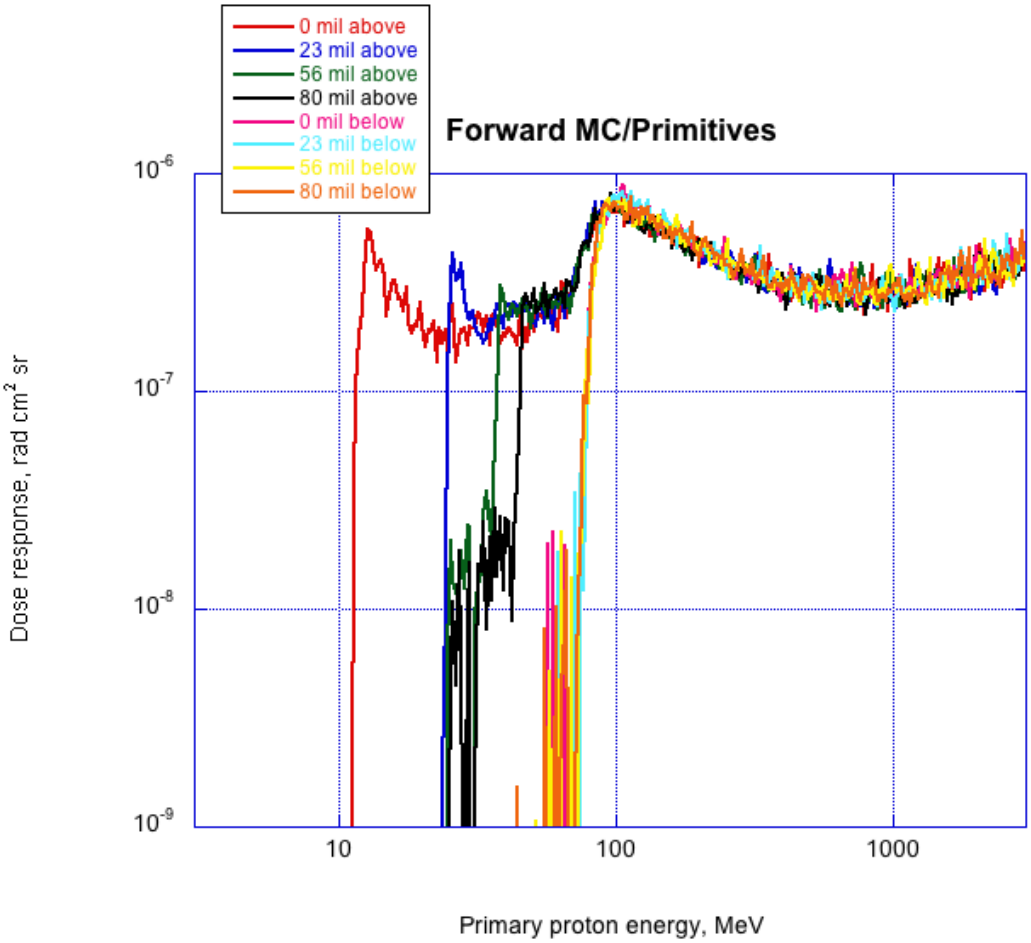

Figure 6. Dose response of microdosimeters with the four Mallory thicknesses, illuminated separately by protons from above and below, for the "Forward MC/Primitives" simulation configuration.

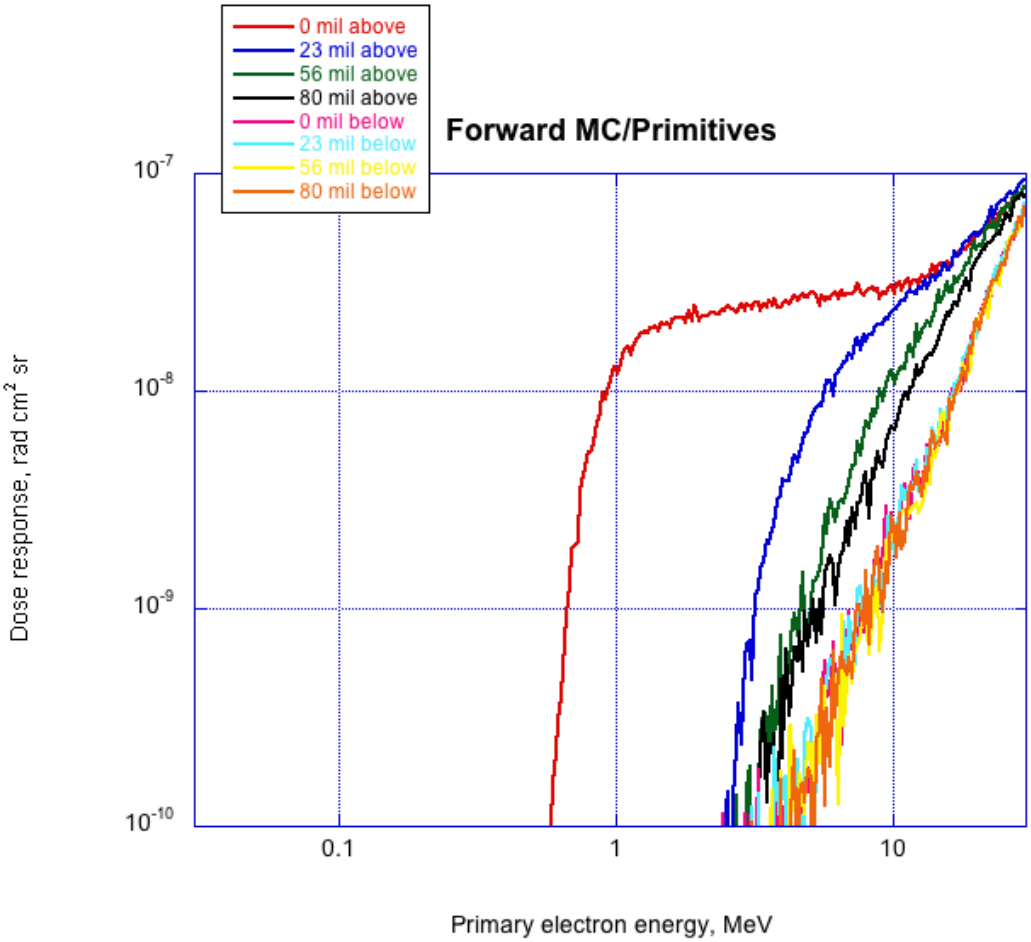

Figure 7. Dose response of microdosimeters with the four Mallory thicknesses, illuminated separately by electrons from above and below, for the "Forward MC/Primitives" simulation configuration.

3. Geometry Imported from CAD Files

Next we redid the forward simulations with the panel, attached structures, and pod housing imported from CAD files rather than built of Geant4 primitives. Figure 8 shows a comparison of runtimes for corresponding primary proton (blue) and electron (red) energies; we divided sets of forward simulations into many runs with different primary particle energies and possibly different numbers of particles, so each point represents the runtime for the same energy and equal numbers of particles in one geometry vs. the other. It can be seen that, for this configuration, having large structures imported from CAD files slows the forward simulation down by about a factor of six. In fact, due to time constraints we ran 1/10 as many particles for the imported geometry as for the all hand-built geometry (Figure 8 is scaled to make the comparison), and so the dose response curves for the imported geometry in Figure 9 and Figure 10 for protons and electrons respectively show significantly more ragged statistics compared to Figure 6 and Figure 7. The agreement within the statistical fluctuations looks good, however, and in other comparisons we have found no apparent artifacts that are introduced by the use of structures imported from CAD files. Thus, if the significant slowdown in runtime is of less importance than the speedup of the coding of the geometry, we are confident in using CAD import as part of our geometries where such files are available at an appropriate level of detail.

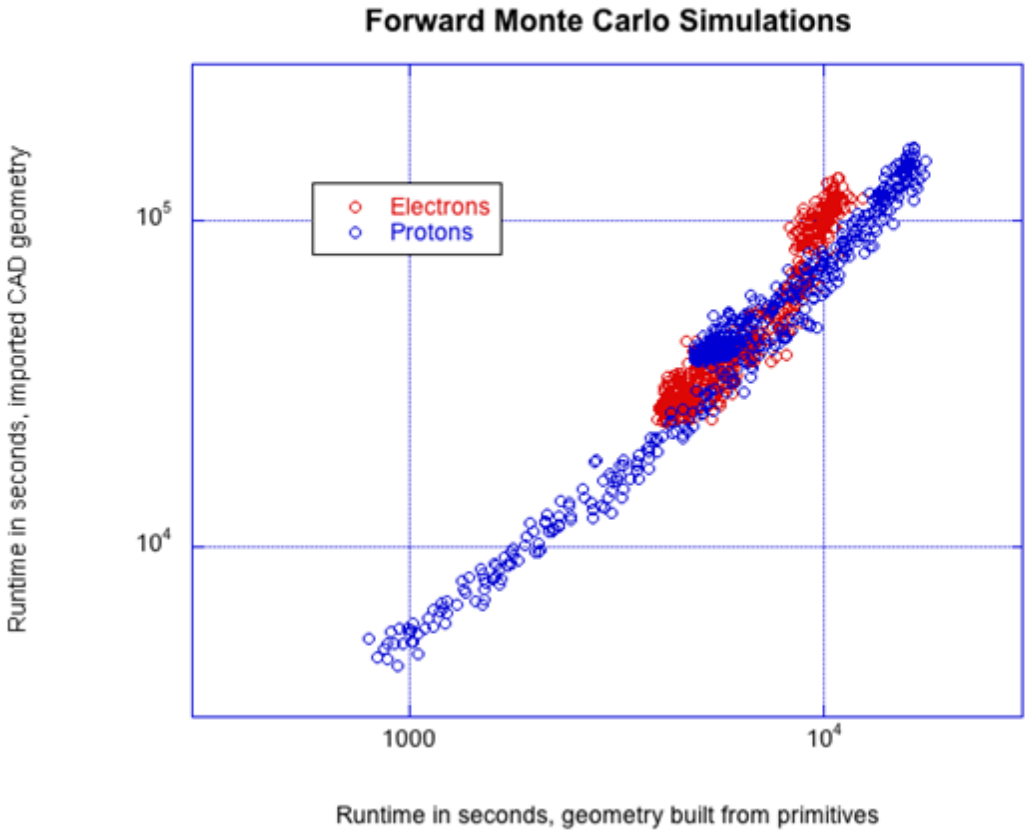

Figure 8. Comparison of runtime for forward Monte Carlo simulations with geometry partially imported from CAD files vs. with all geometry constructed from Geant4 primitives. Blue points are for protons, red for electrons; each point represents an average runtime for an equal number of incident particles at a given primary particle energy in both geometries. Simulations for all pod configurations (Mallory thickness combinations) are compared in this plot.

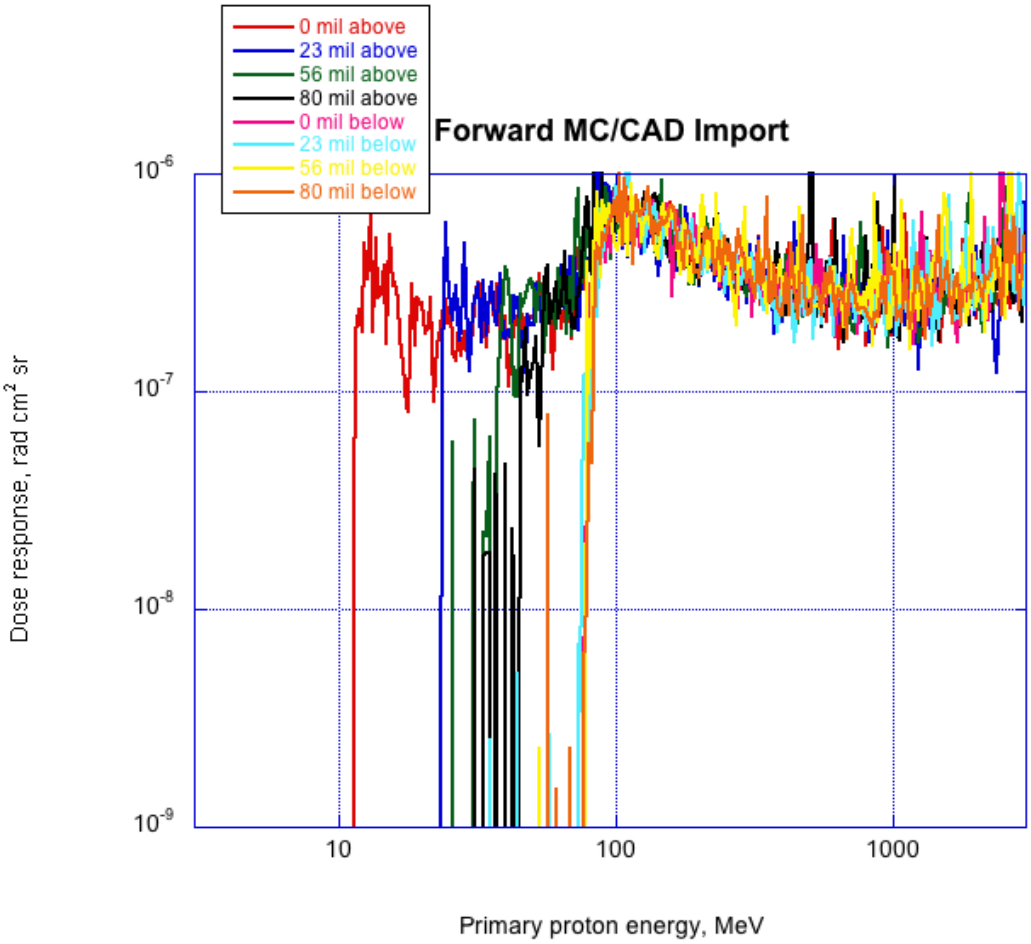

Figure 9. Dose response of microdosimeters with the four Mallory thicknesses, illuminated separately by protons from above and below. "Forward MC/CAD Import" label indicates that these results are for forward Monte Carlo simulations using a geometry with some large structures imported from CAD files. Statistics (number of primary particles simulated at each incident energy) are 1/10 of those in Figure 6, but general agreement looks good.

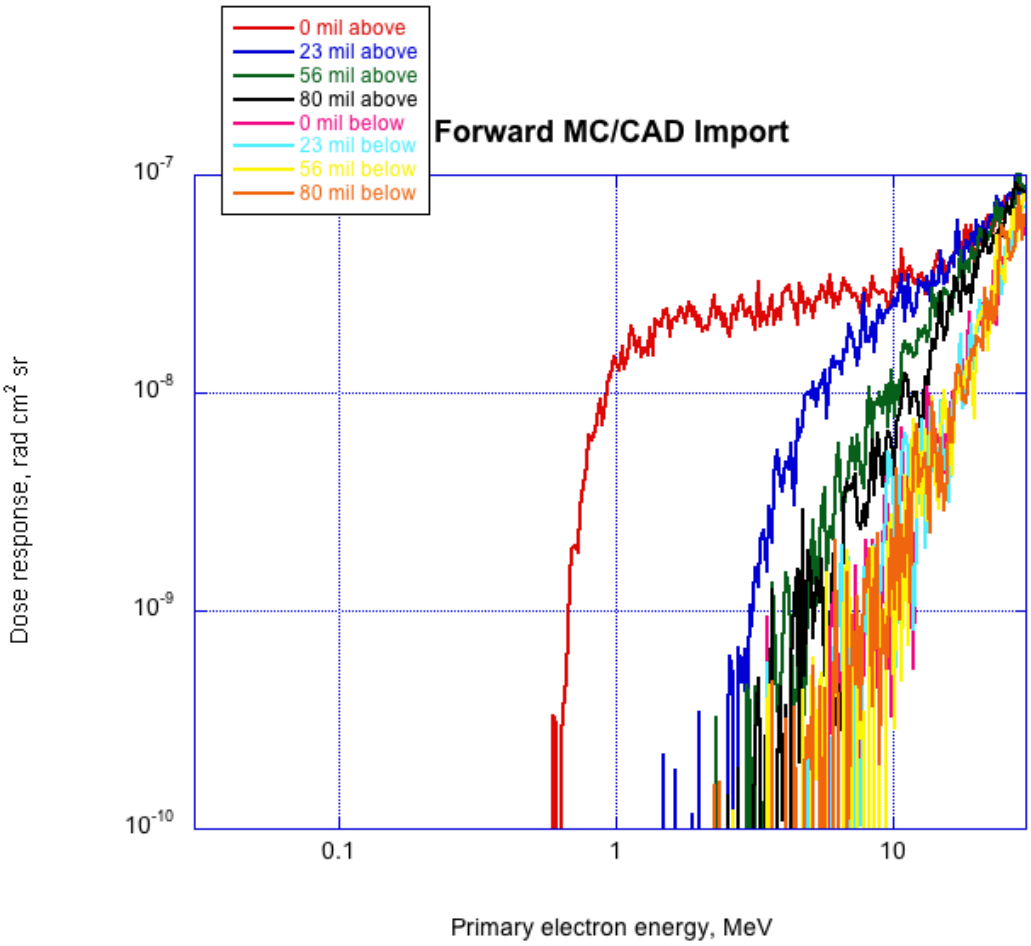

Figure 10. Dose response of microdosimeters with the four Mallory thicknesses, illuminated separately by electrons from above and below, for the "Forward MC/CAD Import" simulations. Again, statistics are 1/10 of those in Figure 7.

4. Adjoint Monte Carlo Simulations

Looper [4] compared forward and adjoint Geant4 Monte Carlo results for a simple test geometry, and found that while electrons agreed well, the adjoint Monte Carlo produced dose that was much too large for energies near where protons would be at or near the end of their ranges in the sensitive volume after traversing different thicknesses of overlying shielding. Individual energy deposits were reasonable. The problem arose with the weights (probability of such an event occurring) assigned to such protons by the adjoint code being too high. In addition, an oscillation of intensity with primary particle energy was seen at higher energies. This is illustrated in Figure 11 to Figure 16, which show the results for the microdosimeter with 0 mils of Mallory and are to be compared to Figure 2 to Figure 7 for the forward Monte Carlo simulations of the same configuration. These figures use the geometry built entirely with Geant4 primitives; we also ran simulations with the geometry partially imported from CAD files, and got very similar results.

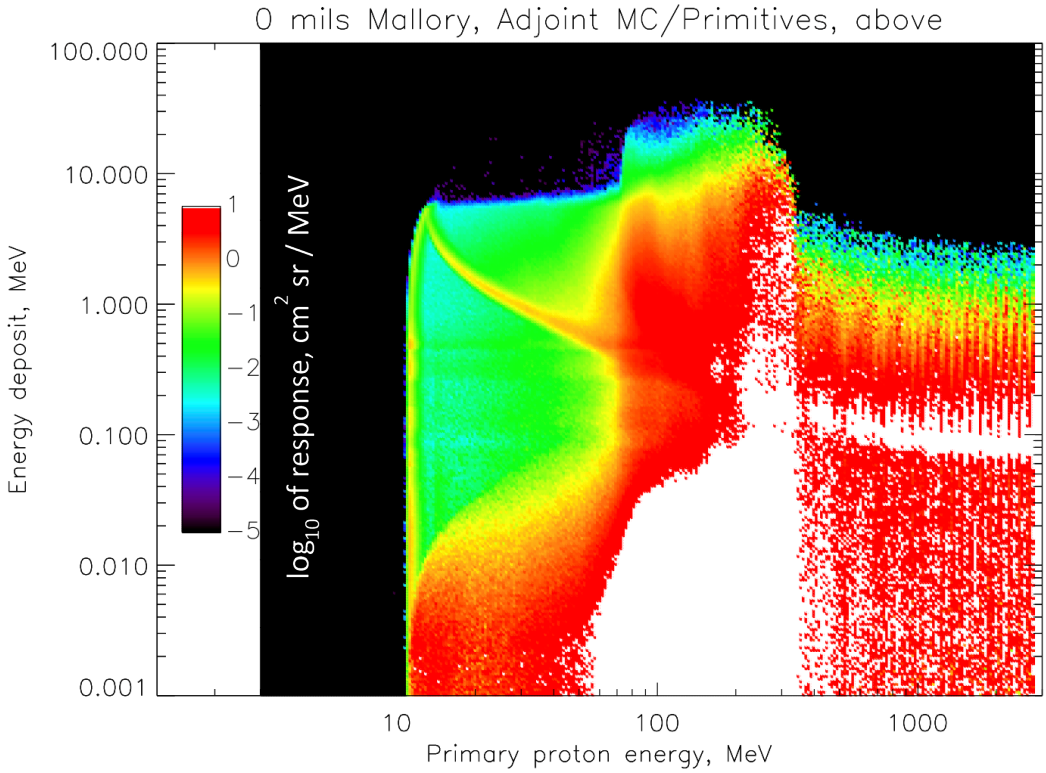

Figure 11. Energy deposit response to isotropically incident protons of microdosimeter without Mallory over aperture. "Adjoint MC/Primitives" indicates adjoint Monte Carlo simulation with geometry built from Geant4 primitives; this plot is for the subset of protons coming in from above the top of the panel to which the REACH pod is mounted. Colorscale is the same as in Figure 2.

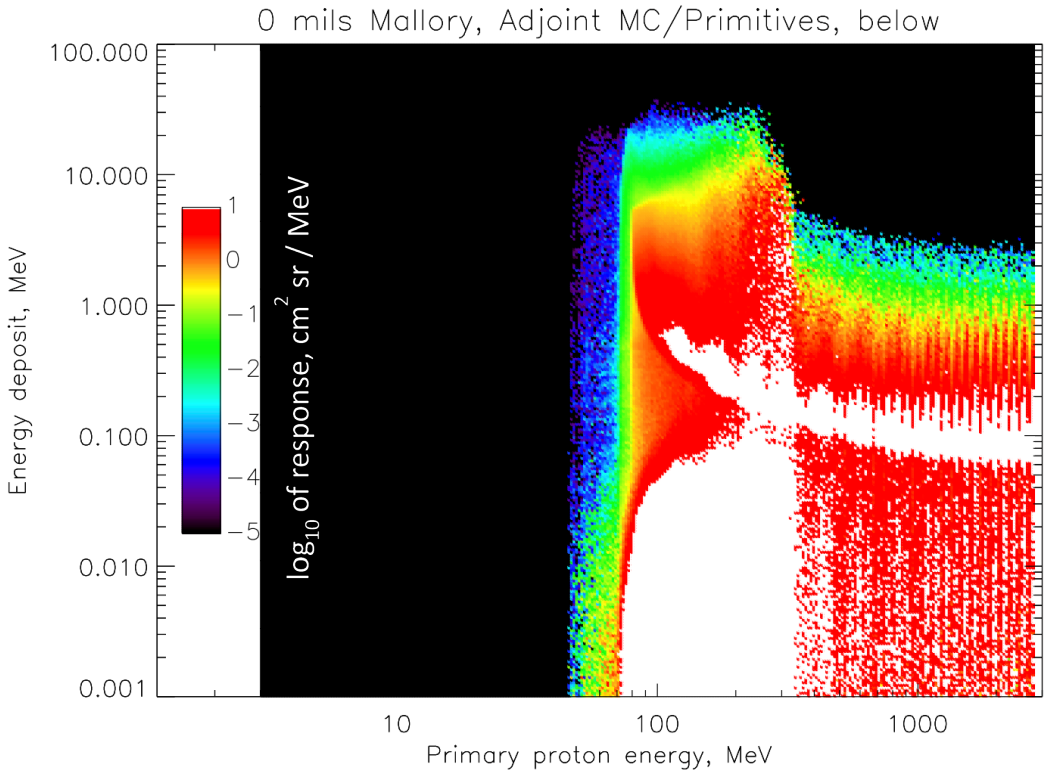

Figure 12. Energy deposit response to isotropically incident protons of microdosimeter without Mallory over aperture. This is the "Adjoint MC/Primitives" simulation configuration, for the subset of protons coming from the rear of the panel. Colorscale is the same as that in Figure 2.

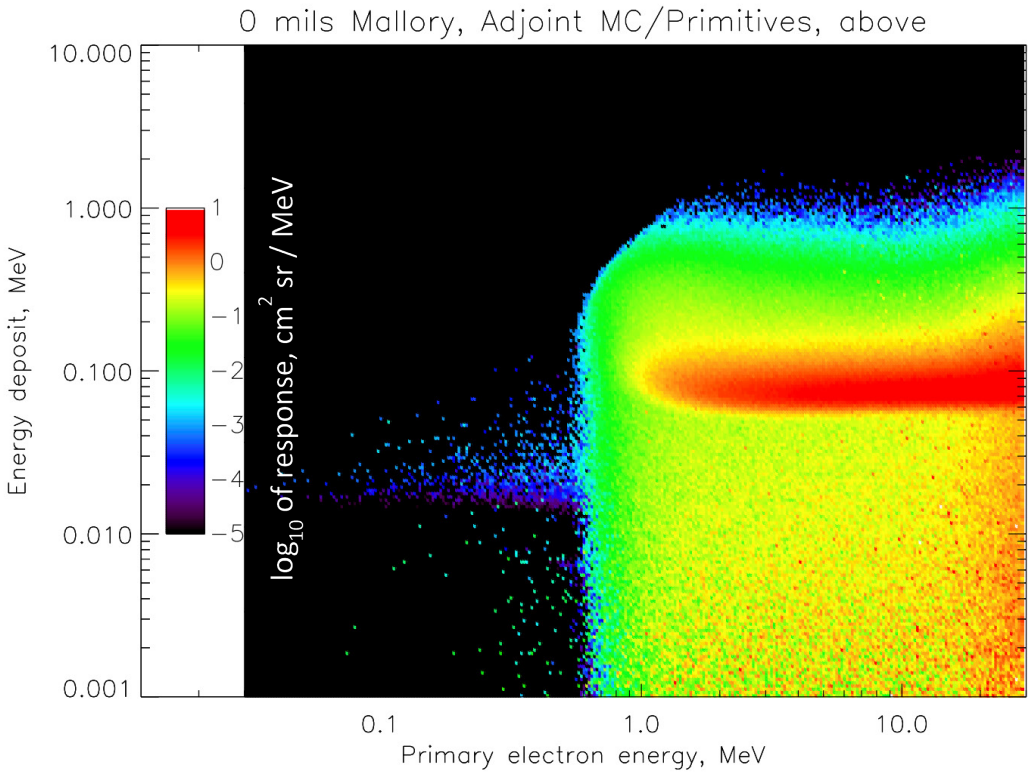

Figure 13. Energy deposit response to isotropically incident electrons of microdosimeter without Mallory over aperture. This is the "Adjoint MC/Primitives" simulation configuration, for the subset of electrons coming from the top of the panel. Colorscale is the same as that in Figure 2.

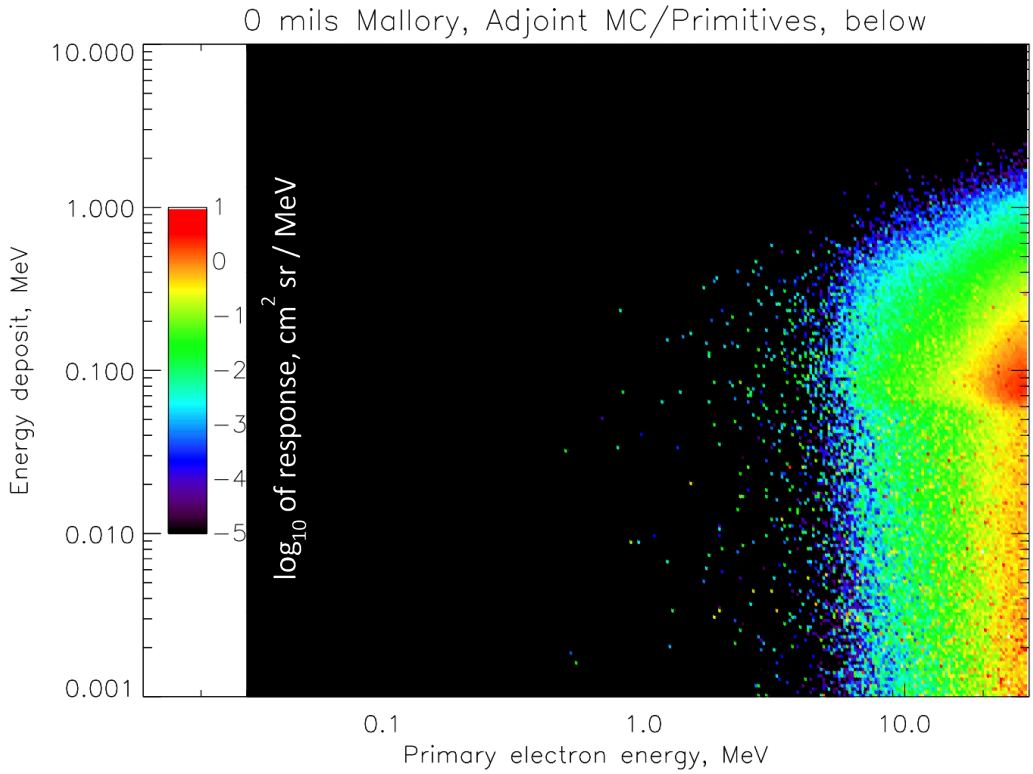

Figure 14. Energy deposit response to isotropically incident electrons of microdosimeter without Mallory over aperture. This is the "Adjoint MC/Primitives" simulation configuration, for the subset of electrons coming from the rear of the panel. Colorscale is the same as that in Figure 2.

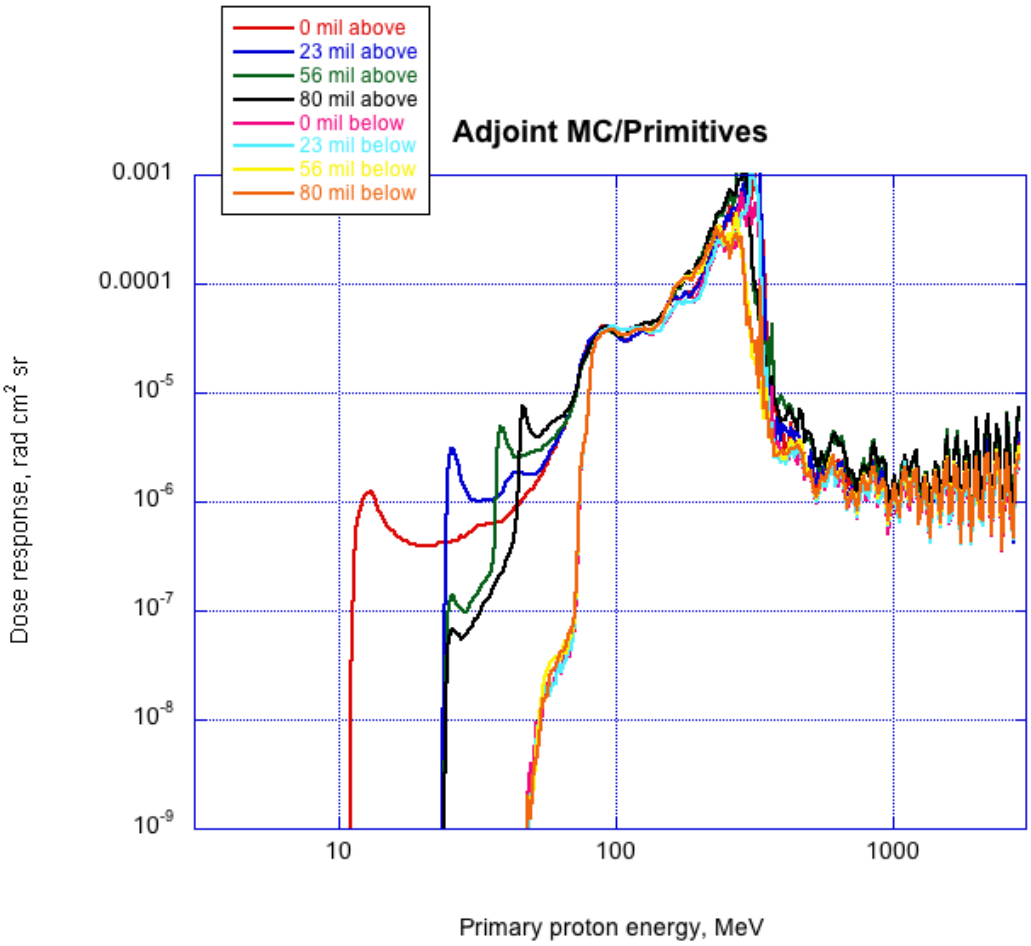

Figure 15. Dose response of microdosimeters with the four Mallory thicknesses, illuminated separately by protons from above and below, for the "Adjoint MC/Primitives" simulations.

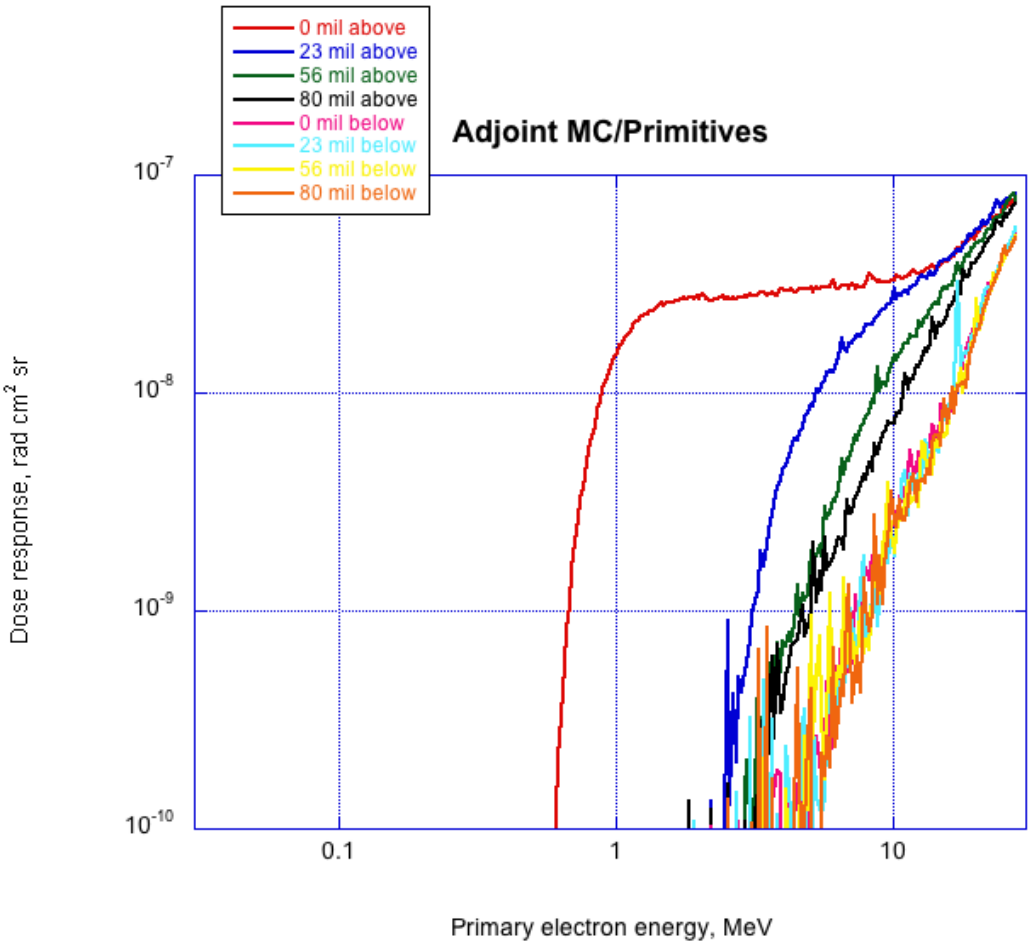

Figure 16. Dose response of microdosimeters with the four Mallory thicknesses, illuminated separately by electrons from above and below, for the "Adjoint MC/Primitives" simulations.

A comparison of timing, as in Figure 8 for the forward simulations, is shown in Figure 17 for the adjoint simulations; it appears that using structures imported from CAD files slows adjoint simulations down less, about a factor of two rather than six or so. A comparison of speed vs. forward simulations for the same number of particles is difficult because a forward simulation launches external primary particles which may hit the target, while an adjoint simulation launches particles backward in time from where they have definitely hit the target; however, comparing the number of energy-deposit events in the forward simulations with the number of particles at the target in the adjoint simulations, we can roughly estimate that the same statistics for such events at the target can be achieved about a hundred times faster via the adjoint technique in this geometry! The contrast would be even greater with a larger overall simulation volume compared to the size of the detector, say the entire host spacecraft. To take advantage of this, we will continue evaluating the Geant4 adjoint Monte Carlo capability as new versions of the code are released; for now, however, we are confident that we can use it for electrons, but not for protons. We do note some spikes along the curves in Figure 15 and Figure 16 for electrons; these are due to the known problem, remarked on in the code documentation, of occasional weights that are too high for gammas at the target in adjoint simulations. We will have to include code to discard such rare outlier events in future adjoint work.

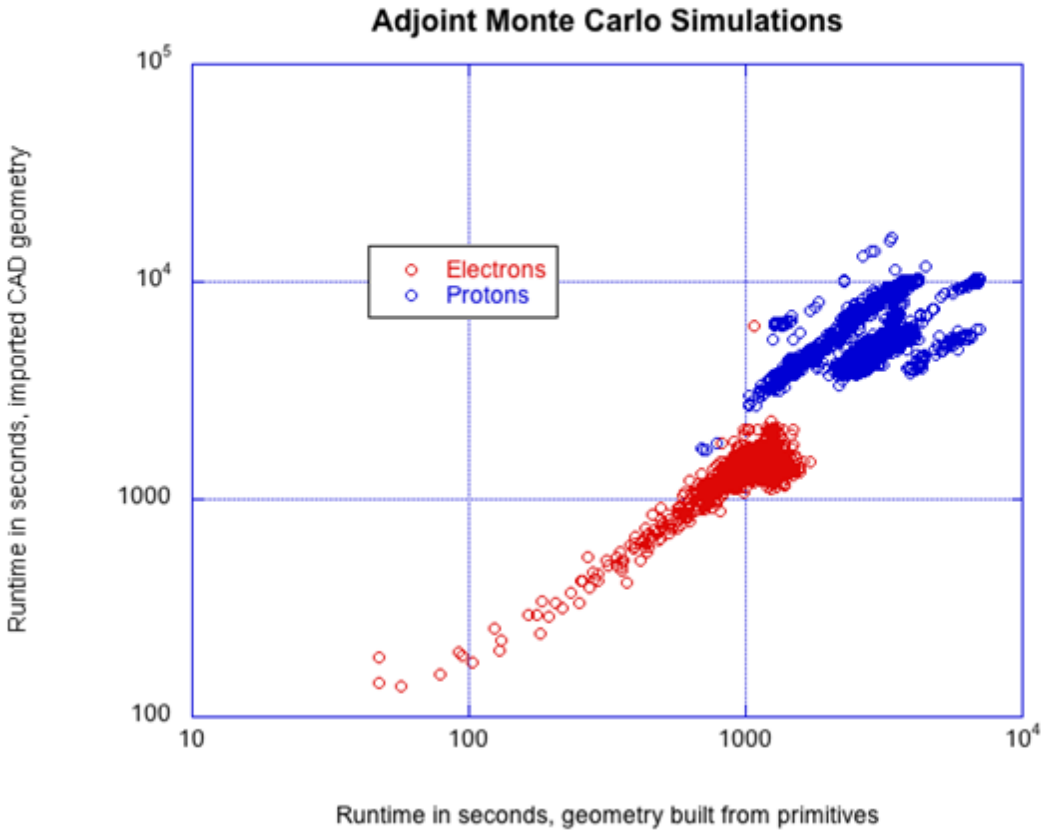

Figure 17. Comparison of runtime for adjoint Monte Carlo simulations with geometry partially imported from CAD files vs. with all geometry constructed from Geant4 primitives. Blue points are for protons, red for electrons; each point represents an average runtime for an equal number of particles launched outward from the detector at a given energy in both geometries. Simulations for all pod configurations (Mallory thickness combinations) are compared in this plot.

5. Improved Sector Shielding Calculation

As an alternative to the adjoint Monte Carlo technique to speed up calculations for protons, Looper [4] modified the standard sector shielding calculation to include variable pathlengths through the detector, rather than a single average dose for each combination of shielding thickness and primary proton energy, and to scale material densities to better represent proton energy loss in each, rather than simply adding column mass densities of all materials traversed. Figure 18 and Figure 19 show the energy deposit spectra vs. primary proton energy calculated using this technique, for the geometry including some structures imported from CAD files; results for the geometry built entirely from Geant4 primitives are very similar. Prominent bands in the upper part of the figure due to particles coming in through particular combinations of inert material (only aluminum panel and Kovar lid, or panel and lid plus Mallory shield around the microdosimeter, etc.) are visible much as they were in Figure 2; much of the fine structure toward the bottom of this plot, however, is due to binning of the pathlengths as tabulated for analysis, with (for example) one stripe due to particles penetrating 0.040 gm/cm^2 of silicon and the next due to particles penetrating 0.039 gm/cm^2.

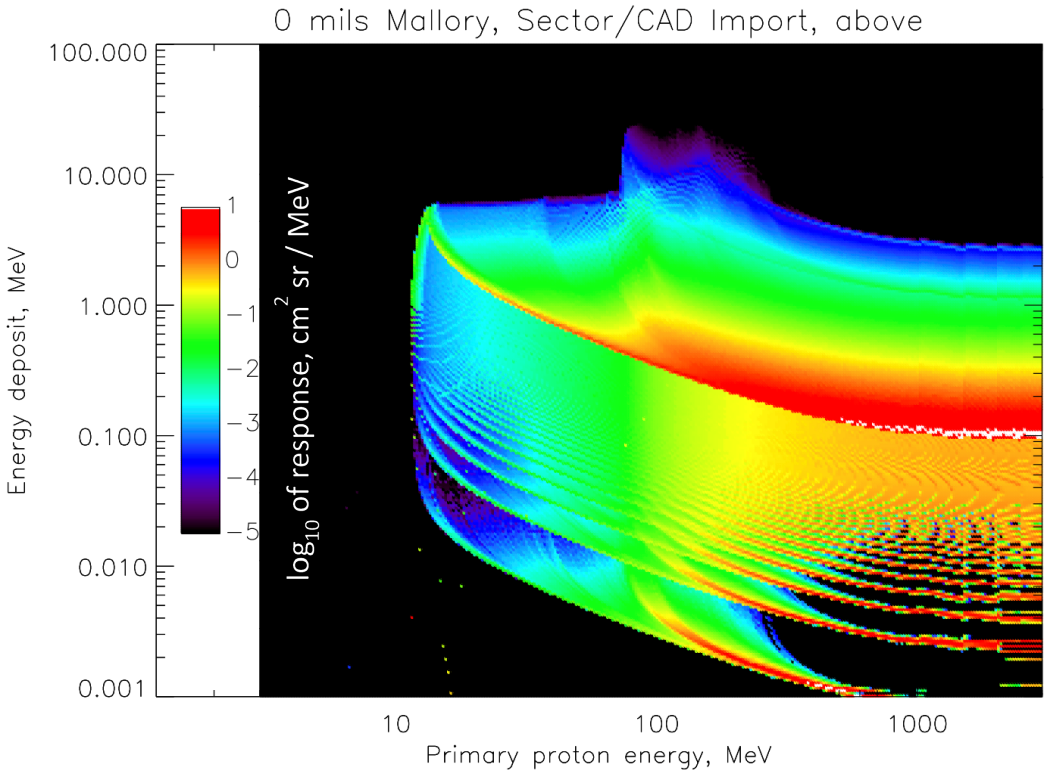

Figure 18. Energy deposit response to isotropically incident protons of microdosimeter without Mallory over aperture. "Sector/CAD Import" indicates modified sector shielding calculation using a geometry with some large structures imported from CAD files; this plot is for the subset of protons coming in from above the top of the panel to which the REACH pod is mounted. Colorscale is the same as that in Figure 2.

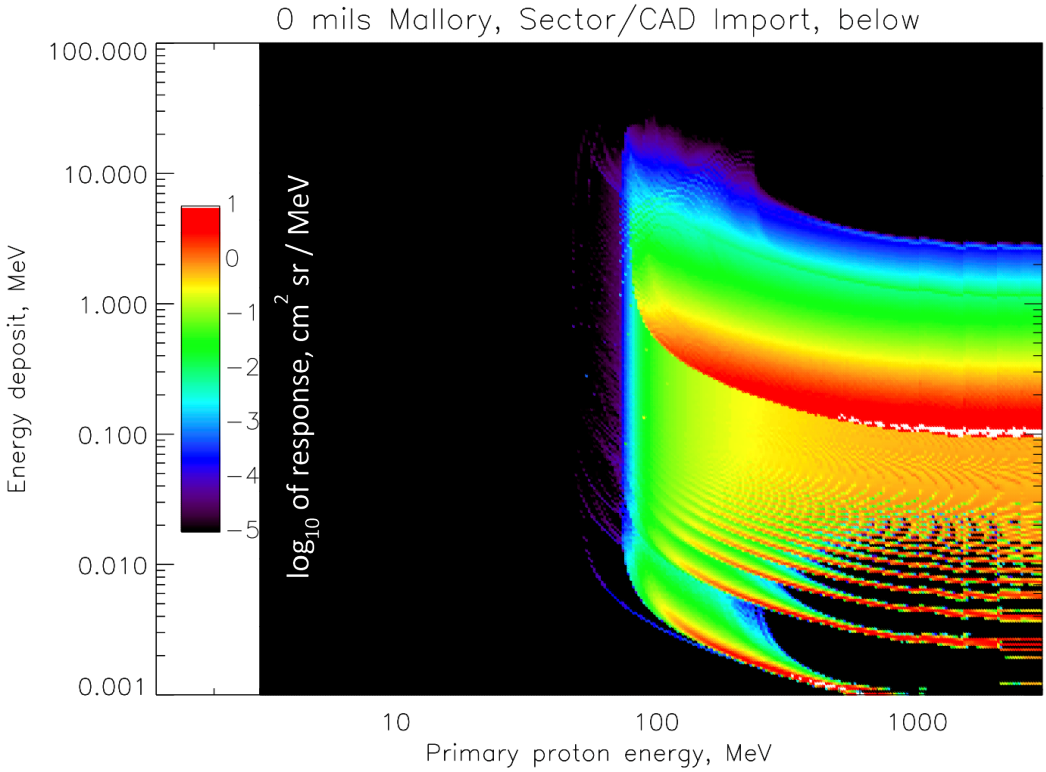

Figure 19. Energy deposit response to isotropically incident protons of microdosimeter without Mallory over aperture. This is the "Sector/CAD Import" simulation configuration, for the subset of protons coming from the rear of the panel. Colorscale is the same as that in Figure 2.

Figure 20 shows the summed dose response for the same configuration, for illumination from above and below of all four Mallory thicknesses. Comparing with Figure 6, we see very similar patterns for most curves and most energies; in particular, steps associated with penetration of different combinations of inert material are in the same places, indicating that the correction to the column density of different materials is having the desired effect (without the correction, all curves shift to higher energies due to the effect of materials heavier than the nominal aluminum). There are two notable differences. First, the primary response between about 35 and 60 MeV for the two greatest Mallory thicknesses (for illumination from above, green and black curves) is about a factor of two too low compared to Figure 6; it is not clear why this is the case, but it probably originates from a single numerical scaling factor (chosen for protons around 100 MeV) having been used to adjust column densities of materials along all paths, and this factor is not close enough to the actual effect of Mallory on these lower-energy protons. Second, these curves do not turn up in the vicinity of several hundred MeV, as do the curves in Figure 6; this is because only electromagnetic physics, encapsulated in a tabulation of range vs. energy (and the correction to that for different materials), are included in this calculation, and so no account is taken of extra dose due to high-Z nuclear fragments reaching the detector after a high-energy proton strikes a target atom. The poorer accuracy at the highest energies would not be a significant effect for REACH because of the spectral shape of typical natural radiation environments.

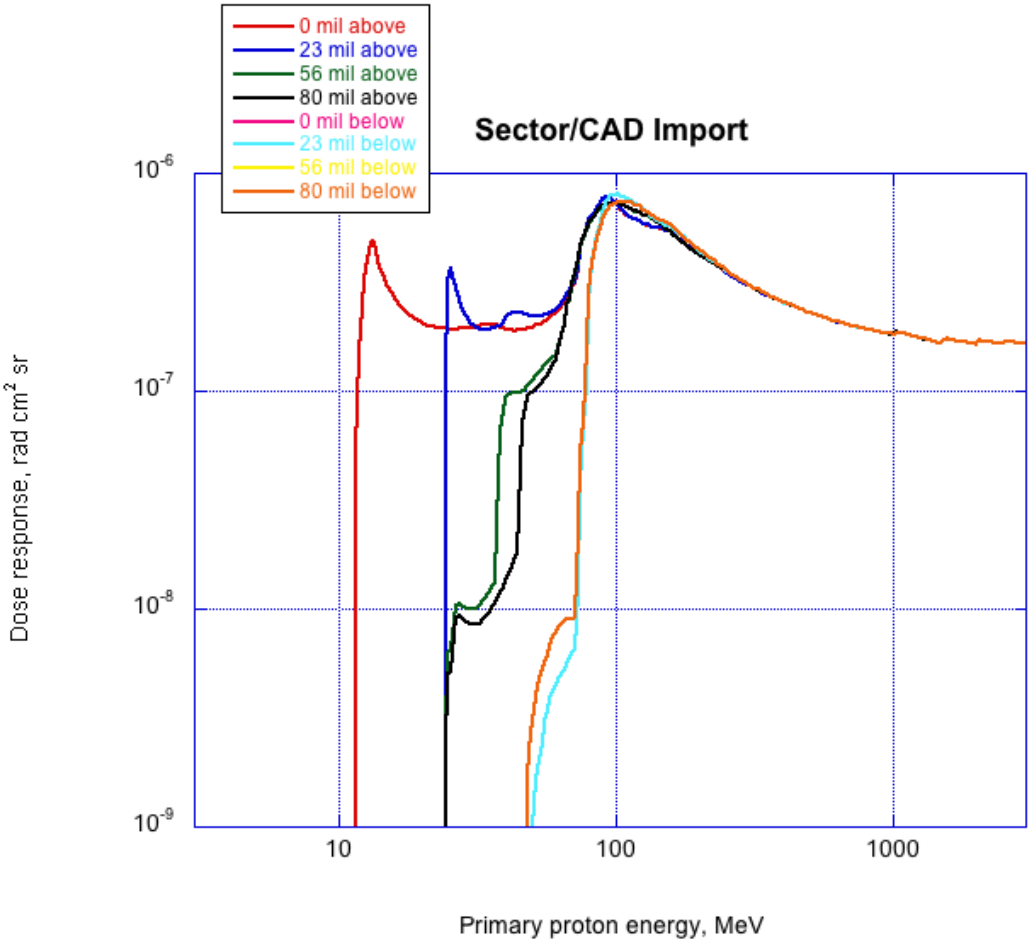

Figure 20. Dose response of microdosimeters with the four Mallory thicknesses, illuminated separately by protons from above and below, with sector shielding calculation and geometry including large structures imported from CAD files.

The missing extra dose due to nuclear interactions means that results from this technique are only valid up to several hundred MeV; beyond that, a dose enhancement factor determined from other calculations, like that in Figure 6, will have to be assumed. The reduced response calculated using this technique for thicker, denser shielding over a detector can be corrected by using the range-energy relation of Mallory (90% tungsten) rather than of aluminum to do the calculation, correcting other materials to match that rather than aluminum. However, for lower energies one can sidestep these physical approximations altogether by performing a full forward Monte Carlo simulation illuminating only the area near the sensitive detector with these lower-energy protons so as to build up statistics more quickly than for a full omnidirectional simulation, and then splicing results from that into the sector shielding calculation of the whole volume for higher energies, as was done by (e.g.) Looper [3] for focused (near-aperture) and omnidirectional forward Monte Carlo simulations of a CubeSat.

Another difference between Figure 6 and Figure 20 is that the curves in Figure 20 are much smoother than those in Figure 6, due to far greater statistics. This was also achieved in much less time: forward or adjoint Monte Carlo simulations with reasonable statistics for a geometry like this take hours or days on hundreds of cluster computing cores, whereas a sector shielding calculation is finished in a few hours on a single desktop computer core. This substantial increase in speed, and also the improved accuracy compared with the current state of Geant4 adjoint Monte Carlo simulations for protons, makes this a useful technique for calculations involving a small sensitive volume inside a large shielding volume, despite the extra work needed to compensate for the limitations of the simpler physics.

Finally, an advantage of our modified sector shielding calculation compared with the standard sector shielding technique is that, for a particular combination of pathlength through shielding and primary proton energy, the energy deposit logged is calculated for the actual pathlength into and through the geometry of the silicon detector. This allows for calculation of a realistic distribution of energy deposits (provided that the spacing of binning bands, as seen in Figure 19, is close enough in the energy-deposit range of interest), rather than the use of an average value for each combination of pathlength and energy regardless of how the incident proton strikes the detector; this in turn enables this technique to be used for calculations involving, for example, an electronic dosimeter threshold such that only energy deposits above a certain level are added to the accumulated dose. A comparison of such a calculation for a 1 MeV threshold (as used in REACH model-1 pods) is presented in Figure 21 and Figure 22, which apply such a cut to the energy deposits that went into Figure 6 and Figure 20 respectively. Subject to the caveats in the discussion above of those figures (especially the absence in Figure 20 of large energy deposits due to nuclear fragments produced at high primary proton energies), the results look very similar.

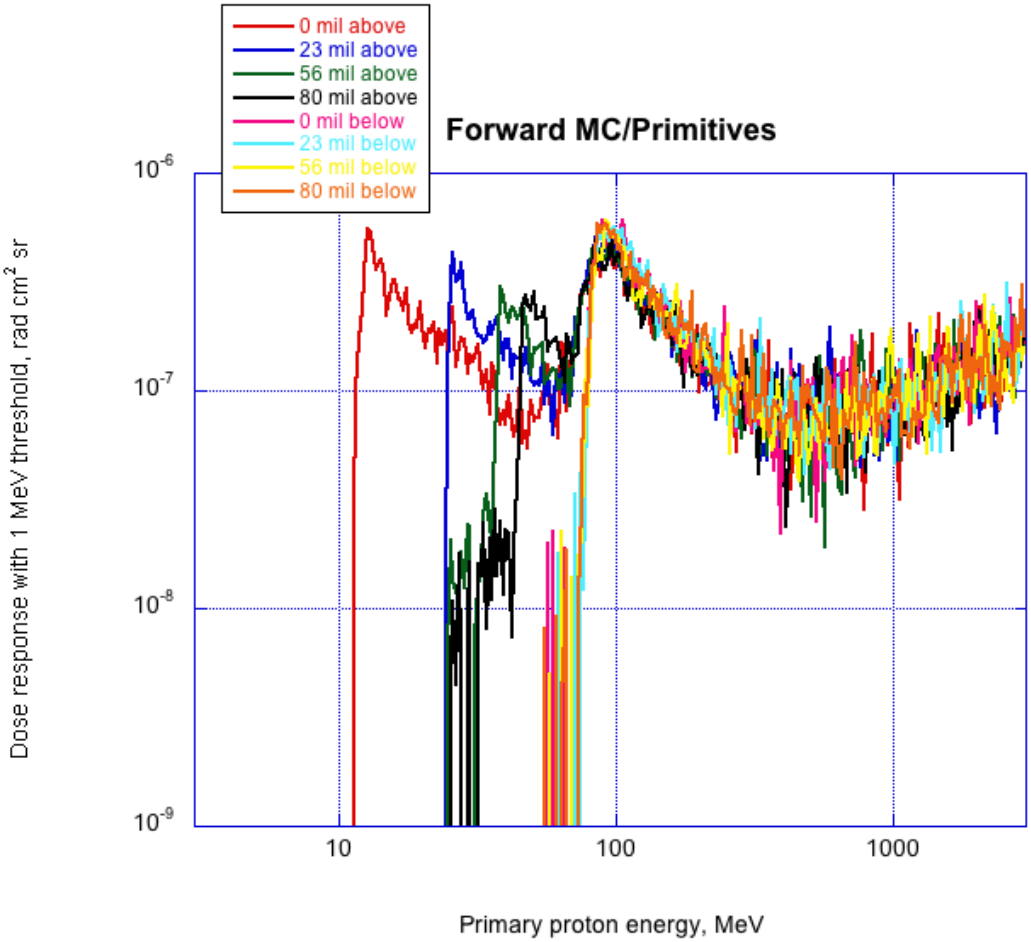

Figure 21. Dose response of microdosimeters with the four Mallory thicknesses, illuminated separately by protons from above and below, for a forward Monte Carlo simulation and geometry built from Geant4 primitives, with a 1 MeV threshold applied to energy deposits before they are added to the dose.

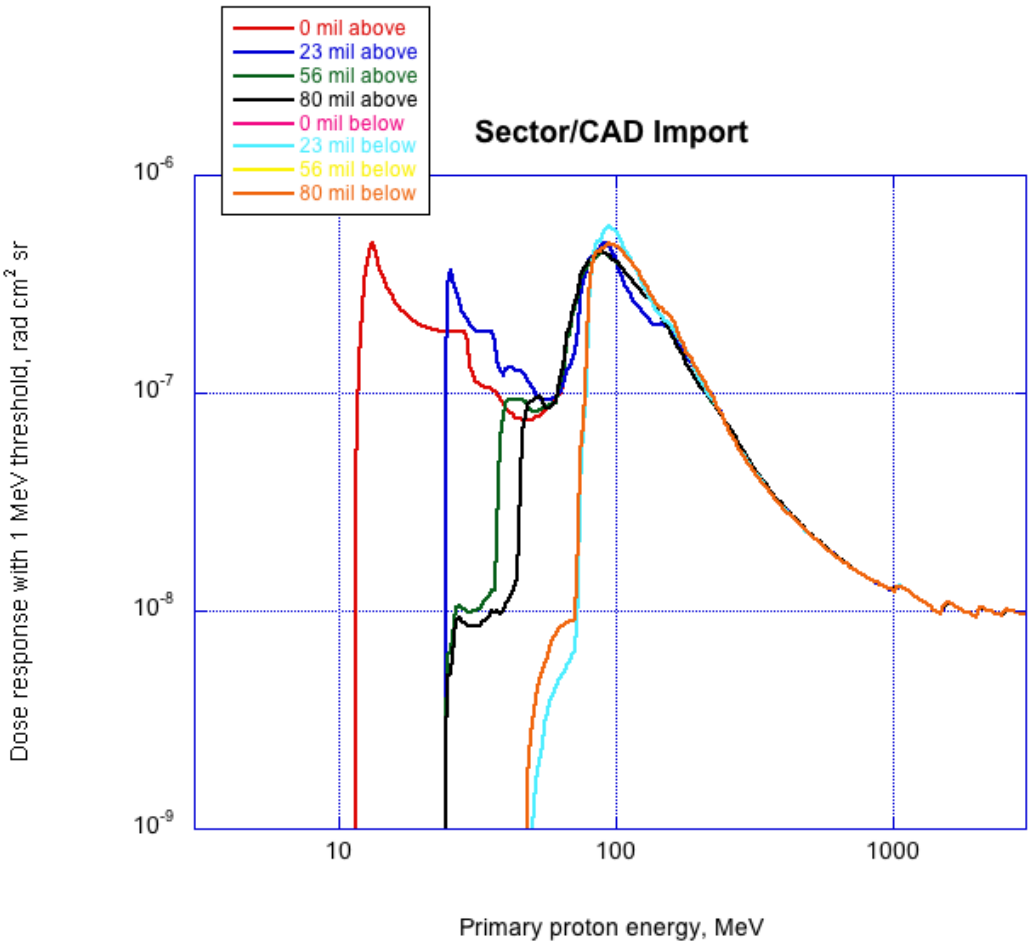

Figure 22. Dose response of microdosimeters with the four Mallory thicknesses, illuminated separately by protons from above and below, for a sector shielding calculation and geometry including large structures imported from CAD files, with a 1 MeV threshold applied to energy deposits before they are added to the dose.

6. Summary and Conclusions

1. Geant4 calculates substantially the same results whether all of the modeled geometry is built from Geant4 primitives, or major portions are imported from CAD files. This conclusion holds true for forward or adjoint Monte Carlo simulations or for sector shielding calculations. Some small differences may be expected due to the approximations necessary in decomposing the complex shapes of actual hardware into Geant4 primitives, but we saw none in our comparisons. Thus it appears that we are using the Geant4 CAD import facility correctly, and we can be confident in using it for larger structures where it is not feasible to break everything down into primitives to check the CAD results, as was done herein.

2. The forward simulation runs about 6x slower with CAD structures than without, and the adjoint simulation about 2x slower, for this specific geometry. Extra runtime will be needed to obtain the same statistics if CAD import of geometry is used.

3. Adjoint Monte Carlo simulations are orders of magnitude faster than forward simulations. It is difficult to compare speeds of forward and adjoint simulations directly with one another, but for this geometry the improvement appears to be around a factor of 100 to get similar numbers of energy-deposit events in the target.

4. For electrons, forward and adjoint Monte Carlo simulations give substantially similar results. Comparing Figure 7 for the forward and Figure 16 for the adjoint simulations of electrons, we see that they are close, with the latter being about 20% higher in places. Occasional spikes due to rare events assigned too high a weight, as is remarked on in the Geant4 code package's documentation, will need to be removed by identification and elimination of these outlier events. On the whole, though, these small differences appear to be acceptable tradeoffs in order to greatly speed up a calculation like this.

5. For protons, the present state of the Geant4 adjoint Monte Carlo simulation gives results with differences from forward simulations that are too large to be acceptable.

6. Our improved sector shielding technique is a suitable substitute for an adjoint simulation, in the case of proton calculations for which a forward Monte Carlo simulation would be too slow. As an alternative to an adjoint simulation for protons, we have developed an improved sector shielding calculation that accounts for different pathlengths through the sensitive detector for different incidence directions and locations, and that corrects the column densities of different materials to account for their different effects on proton energy loss compared to aluminum. This is extremely fast compared to either forward or adjoint Monte Carlo simulations. Like the latter, it does not account for nuclear interactions enhancing the dose from high-energy primary protons; it can also show artifacts for paths through the inert structure consisting mostly of materials other than the nominal aluminum. These artifacts can be corrected by choosing another nominal material for the range-energy calculation and simply using different scaling factors to relate other materials' column densities to the new nominal material. Alternatively, results from a focused forward Monte Carlo simulation illuminating just the area around the sensitive detector(s) can be spliced in to replace these parts of the calculation, as demonstrated by Looper [3]. With these caveats, this technique appears to be an acceptable way to speed up calculations of proton response, and the improvements relative to the standard point sector shielding calculation also enable its use for calculations that need a realistic distribution of energy deposits, rather than averages.

In general, a forward Monte Carlo simulation will give the most accurate results. For geometries with sensitive volumes that are small compared with the inert material around them, a Geant4 adjoint Monte

Carlo simulation will give good results for electrons with much less computational time, and our improved sector shielding technique will do the same for protons. Accuracy of the overall calculation can be improved by letting the adjoint or sector shielding techniques calculate response for particles coming in through the bulk of the inert material, and replacing the portions of the response due to particles entering the geometry through thinner material near the sensitive volume (an aperture if one is defined, or just the thinnest part of the shielding) with the response derived from a forward Monte Carlo simulation illuminating just this portion of the geometry, for better statistics. We have performed and are analyzing the results of just such a combination of calculations for the full REACH geometry aboard a mass model of its host spacecraft. The geometry of the payload into which the REACH pod is integrated was constructed by import from CAD files (of which a subset was used for the comparison herein), and a simple mass model of the spacecraft was built from Geant4 primitives. We will prepare a separate report on the results, with restricted distribution due to the proprietary information necessary for the full modeling.

7. References

1. Allison, J., *et al*. (2016), "Recent Developments in Geant4," *Nucl. Instrum. Methods Phys. Res. A* 835, 186-225, doi: 10.1016/j.nima.2016.06.125

2. Chytracek, R., J. McCormick, W. Pokorski, and G. Santin (2006), "Geometry Description Markup Language for Physics Simulation and Analysis Applications," *IEEE Trans. Nucl. Sci*. 53 (5), 2892-2896, doi: 10.1109/TNS.2006.881062

3. Looper, Mark D. (2016), "Updated Geant4 Simulations of AeroCube 6 Microdosimeters," TOR-2016-03260.

4. Looper, Mark D. (2018), "Adjoint Monte Carlo Simulations and Improved Sector Shielding Calculations with Geant4," ATR-2018-00052

5. Looper, M. D., *et al*. (2013), "The Radiation Environment Near the Lunar Surface: CRaTER Observations and Geant4 Simulations," *Space Weather* 11 (4), 142-152, doi: 10.1002/swe.20034

6. O'Brien, T. P., J. E. Mazur, T. B. Guild, and M. D. Looper (2015), "Using Polar-orbiting Environmental Satellite Data to Specify the Radiation Environment up to 1200 km Altitude," *Space Weather* 13, 433-445, doi: 10.1002/2015SW001166

External Distribution

REPORT TITLE

Comparison of Modeling Techniques for Radiation Dose in a Realistic Geometry

REPORT NO.	PUBLICATION DATE	SECURITY CLASSIFICATION
ATR-2018-00953	February 28, 2018	UNCLASSIFIED

Capt. Felix A. Abeyta
USAF
felix.abeyta.1@us.af.mil

Makoto Asai
Stanford Linear Accelerator Center
asai@slac.stanford.edu

Robin J. Barnes
Johns Hopkins University
Applied Physics Laboratory
Robin.Barnes@jhuapl.edu

Laurent Desorgher
Centre Hospitalier Universitaire Vaudois
Laurent.Desorgher@chuv.ch

Michael A. Kelly
Johns Hopkins University
Applied Physics Laboratory
Michael.Kelly@jhuapl.edu

Tom Sotirelis
Johns Hopkins University
Applied Physics Laboratory
Tom.Sotirelis@jhuapl.edu

Insoo Jun
JPL
insoo.jun@jpl.nasa.gov

Release to Public	Control Export
Yes ☑ No ☐	Yes ☐ No ☑

APPROVED BY_____ DATE_____
(AF OFFICE)

AEROSPACE REPORT NO.
ATR-2018-00953

Comparison of Modeling Techniques for Radiation Dose in a Realistic Geometry

Approved Electronically by:

James L. Roeder,
DIRECTOR
SPACE SCIENCES
DEPARTMENT
SPACE SCIENCE
APPLICATIONS
LABORATORY
ENGINEERING &
TECHNOLOGY GROUP

James H. Clemmons, PRINC
DIRECTOR
SPACE SCIENCE
APPLICATIONS
LABORATORY
PHYSICAL SCIENCES
LABORATORIES
ENGINEERING &
TECHNOLOGY GROUP

Lynn M. Friesen, PRINC
DIRECTOR
OFFICE OF PRODUCT
MANAGEMENT
TECHNOLOGY &
LABORATORY
OPERATIONS
ENGINEERING &
TECHNOLOGY GROUP

Cognizant Program Manager Approval:

Margaret W. Chen, ASSOC DIRECTOR
SPACE SCIENCES DEPARTMENT
SPACE SCIENCE APPLICATIONS LABORATORY
ENGINEERING & TECHNOLOGY GROUP

Aerospace Corporate Officer Approval:

Charles L. Gustafson, SR VP ENG & TECH
ENGINEERING & TECHNOLOGY GROUP

SL0345

AEROSPACE REPORT NO.
ATR-2018-00953

Comparison of Modeling Techniques for Radiation Dose in a Realistic Geometry

Content Concurrence Provided Electronically by:

Mark D. Looper, RES SCIENTIST
MAGNETOSPHERIC & HELIOSPHERIC SCIENCES
SPACE SCIENCES DEPARTMENT
ENGINEERING & TECHNOLOGY GROUP

Technical Peer Review Performed by:

T Paul O'Brien, RES SCIENTIST
AVIR MAGNETOSPHERIC & HELIOSPHERIC SCI
SPACE SCIENCES DEPARTMENT
ENGINEERING & TECHNOLOGY GROUP

Office of General Counsel Approval Granted Electronically by:

Domenic C. Rigoglioso, ASSOC GEN COUNSEL
OFFICE OF THE GENERAL COUNSEL
OFFICE OF GENERAL COUNSEL & SECRETARY

Export Control Office Approval Granted Electronically by:

Edward Pevzner, EXPORT CONTROL STAFF IV
GOVERNMENT SECURITY
SECURITY OPERATIONS

SL0345